A safe and cost-effective PMMA carbon source for MgB$_2$

Mahipal Ranot[a], S. H. Jang[c], K. P. Shinde[b], B. B. Sinha[d], A. Bhardwaj[e], Y.-S. Oh[a], S. H. Kang[a], and K. C. Chung[*,b]

[a] Materials Deformation Department, Korea Institute of Materials Science, Changwon 51508, Republic of Korea
[b] Functional Nano Powder Materials Department, Korea Institute of Materials Science, Changwon 51508, Republic of Korea
[c] Kiswire Advanced Technology Ltd, Daejeon, Republic of Korea
[d] National Centre for Nanoscience and Nanotechnology, University of Mumbai, Mumbai 400098, India
[e] Department of Physics, Sungkyunkwan University, Suwon 440-746, Republic of Korea

Abstract

Carbon is proven to be very effective in pinning the magnetic vortices and improving the superconducting performance of MgB$_2$ at high fields. In this work, we have used polymethyl methacrylate (PMMA) polymer as a safe and cost effective carbon source. The effects of molecular weight of PMMA on crystal structure, microstructure as well as on superconducting properties of MgB$_2$ were studied. X-ray diffraction analysis revealed that there is a noticeable shift in (100) and (110) Bragg reflections towards higher angles, while no shift was observed in (002) reflections for MgB$_2$ doped with different molecular weights of PMMA. This indicates that carbon could be substituted in the boron honeycomb layers without affecting the interlayer interactions. As compared to undoped MgB$_2$, substantial enhancement in $J_c(H)$ properties was obtained for PMMA-doped MgB$_2$ samples both at 5 K and 20 K. The enhancement could be attributed to the effective carbon substitution for boron and the refinement of crystallite size by PMMA doping.

Keywords: PMMA, MgB$_2$, superconducting properties

1. INTRODUCTION

To increase the potential use of MgB$_2$ superconductor in practical applications the improvements in its critical current density (J_c) under high magnetic fields have to be realized [1, 2]. For this purpose, substitution of carbon (C) from C containing nanomaterials into boron (B) sites of MgB$_2$ lattice has been proven to be very effective [3, 4]. However, the C containing nanomaterials are expensive and they lead to deterioration of self-field and low-field region critical current density of MgB$_2$ due to strong current carrier scattering and current-blocking effects on grain boundaries. To solve this problem and to achieve uniform distribution of C in MgB$_2$, researchers have obtained C coating on B precursor powders using gaseous hydrocarbon (C$_x$H$_y$) sources in RF plasma techniques [5, 6]. However, these hydrocarbon gases are explosive and the RF plasma techniques are complex. Recently, various kinds of polymers have been used as safe solid carbon sources for growth of graphene [7]. In addition, these polymers are inexpensive, non-toxic and easy to handle. Therefore, we chose polymethyl methacrylate (PMMA) polymer, which contains repeating chain of monomeric units of methyl methacrylate. Park *et al.* doped PMMA in MgB$_2$ wires through a wet mixing process and they have reported only some preliminary results [8]. In this work, we have studied

the influence of molecular weight of PMMA on crystal structure, microstructure and superconducting properties of MgB$_2$, with the expectation that the length of the polymer chain (on which molecular weight depends) can have different role in releasing and substitution of C at B sites of MgB$_2$.

2. EXPERIMENTAL

PMMA powder of different molecular weights, M$_w$ ~ 350,000 = 350 kg/mol and 996,000 = 996 kg/mol were used to prepare PMMA-doped MgB$_2$ bulk samples. PMMA 5 wt.% of (Mg + 2B) was dissolved in N,N-dimethyl formamide (DMF). Then, boron powder was thoroughly homogenized in as-prepared PMMA solution. The boron/PMMA/DMF solution was drop-cast on Si wafer and dried at 110 °C for 1 h in vacuum drying oven. The coating of carbon on boron powders was anticipated by decomposition of PMMA at 500 °C for 3 h under Ar atmosphere. Then, the appropriate amount of Mg was properly milled with boron/PMMA composite. The mixed powders were pelletized under 10 t pressure using hydraulic press. A reference undoped MgB$_2$ pellet was also prepared for comparison. The pellets were put into Fe tubes and sintered *in situ* at a temperature of 700 °C for 30 min under the flow of high-purity Ar gas (5N). Finally, the

---

* Corresponding author email: kcchung@kims.re.kr

undoped and PMMA-doped samples were cooled down to room temperature in a continuous flow of Ar gas.

The crystal structures of undoped and PMMA-doped MgB$_2$ samples were investigated by X-ray diffraction (Rigaku, D/Max 2500) using Cu Kα as an X-ray source. The microstructures of samples were examined by field emission scanning electron microscopy (FESEM). The magnetization measurements were carried out on all samples by using a quantum design vibrating sample magnetometer option (Quantum Design PPMS). The superconducting transition temperature (T_c) was obtained from zero-field-cooled (ZFC) measurement by first cooling the sample in zero field and then measuring the magnetic moment as the sample was warmed up in the field of 10 Oe. To estimate the critical current density, the magnetization hysteresis ($M-H$) loops were measured on all samples with magnetic field varying from -9 T to 9 T applied parallel to the longest dimension of the samples.

3. RESULTS AND DISCUSSION

The X-ray diffraction (XRD) patterns for undoped and MgB$_2$ doped with different molecular weights of PMMA are shown in Fig. 1. The MgB$_2$ diffraction peaks are clearly observed along with MgO peaks. From XRD patterns, it is observed that as compared to undoped MgB$_2$ the PMMA-doped MgB$_2$ samples show a noticeable shift in (100) and (110) Bragg reflections towards higher angles as shown more clearly for (110) in the inset of Fig. 1, while no shift was observed in (002) reflections. The shift in angle values is given in Table 1. It indicates that the 'a' lattice parameter was decreased for doped MgB$_2$, while the 'c' parameter remains unchanged, which implies that C could be substituted in the B honeycomb layer without affecting the interlayer interactions. In order to estimate the actual level of C substitution for PMMA-doped samples we used the relation, $x = 7.5 \times \Delta(c/a)$, where x is the composition of C corresponding to the formula Mg(B$_{1-x}$C$_x$)$_2$ and $\Delta(c/a)$ is

TABLE 1
THE 2Θ, SHIFT IN ANGLE, LEVEL OF C SUBSTITUTION, AND CRYSTALLITE SIZE (D) OF UNDOPED AND MgB$_2$ DOPED WITH DIFFERENT MOLECULAR WEIGHTS OF PMMA.

Sample	2Θ$_{100}$	Shift (2Θ)	2Θ$_{002}$	Shift (2Θ)	C level	D size (nm)
Undoped	59.94	0.00	51.83	0.00	0.000	18.0
M$_w$ ~ 350 kg/mol	60.16	0.22	51.84	0.01	0.027	14.5
M$_w$ ~ 996 kg/mol	60.09	0.15	51.84	0.01	0.019	14.0

the change in c/a compared to undoped sample [9]. The C substitution level was observed to be 0.027 and 0.019 for 350 kg/mol and 996 kg/mol PMMA-doped MgB$_2$, respectively. It indicates that more C is released and substituted into MgB$_2$ lattice from lower molecular weight of PMMA. The crystallite size for all samples were calculated by using Scherrer's formula, D $= 0.9\lambda/\beta\cos\theta$, where λ is the X-ray wavelength, θ is a Bragg reflection angle and β is the full width at half maximum (FWHM) [10]. The crystallite size was estimated to be 18 nm for undoped MgB$_2$ and 14.5, 14 nm for MgB$_2$ doped with different molecular weights of 350 kg/mol, 996 kg/mol PMMA, respectively. This shows that the crystallite size is decreased, and the decrease in crystallite size is similar for both PMMA-doped MgB$_2$ samples.

Fig. 2 shows the temperature dependence of magnetization for undoped and PMMA-doped MgB$_2$ with different molecular weights of PMMA. The superconducting transition temperature (T_c) of 37.3 K was obtained for undoped MgB$_2$. When MgB$_2$ was doped with different molecular weights of PMMA, a systematic decrease in T_c was observed with lowering the molecular weight of PMMA. The T_c of 34.9 K was observed for 350 kg/mol PMMA-doped MgB$_2$ sample, which is suppressed by 2.4 K from that of undoped MgB$_2$. The drop in T_c for
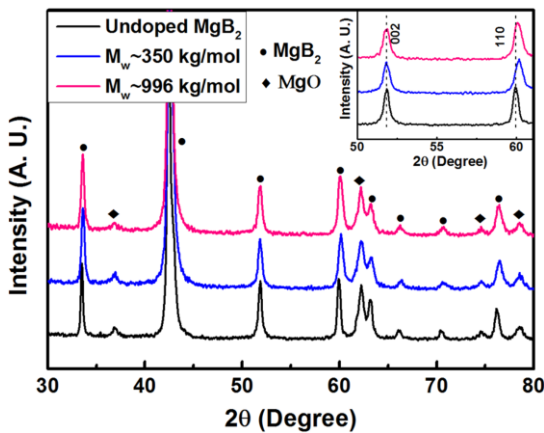

Fig. 1. X-ray diffraction patterns of undoped and MgB$_2$ doped with different molecular weights of PMMA. The inset shows the enlarged view of (002) and (110) Bragg reflections of all samples.
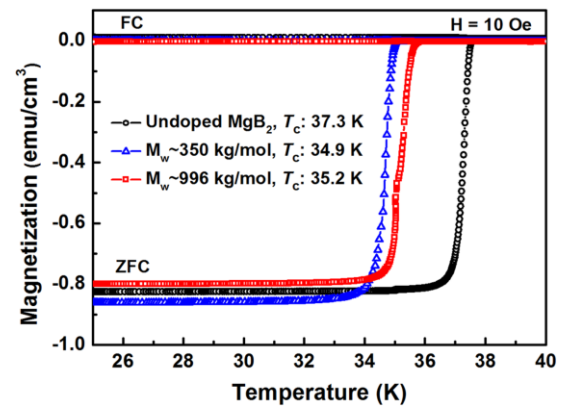

Fig. 2. Temperature dependence of magnetization measured in an applied field of 10 Oe for undoped and MgB$_2$ doped with different molecular weights of PMMA. A decrease in T_c was noticed for PMMA-doped MgB$_2$ samples.
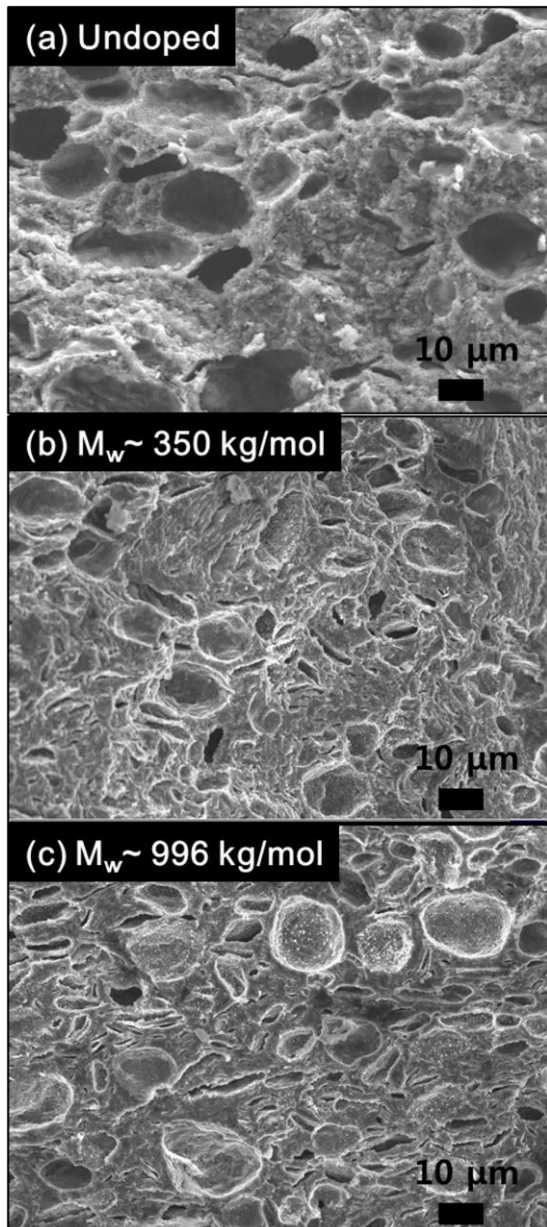
Fig. 3. The FESEM morphologies of (a) undoped and different molecular weights of PMMA (b) 350 kg/mol, and (c) 996 kg/mol doped MgB$_2$ samples.

Fig. 4. The critical current density as a function of magnetic field for undoped and MgB$_2$ doped with different molecular weights of PMMA measured at 5 K (closed symbols) and 20 K (open symbols). As compared to undoped MgB$_2$ significantly high J_c values were observed for PMMA-doped MgB$_2$ samples.

melting of Mg powders during sintering process [13].

To estimate the critical current density, the magnetization (M) as a function of applied field (H) at different temperatures was measured for all samples. The J_c was estimated by Bean's critical state model, $J_c = 20\Delta M/a(1\text{-}a/3b)$, where ΔM is the height of the M–H loop, a and b are the thickness and width of the sample, respectively. The critical current density as a function of magnetic field for undoped and PMMA-doped MgB$_2$ samples measured at 5 K and 20 K are shown in Fig. 4. At 20 K, in the self-field and low-field region, the J_c's of undoped and 996 kg/mol PMMA-doped MgB$_2$ samples almost overlap with each other, whereas 350 kg/mol PMMA-doped sample shows slightly low 'J_c' values. However, in the high-field region this sample shows a cross-over with undoped and 996 kg/mol PMMA-doped MgB$_2$ at 2 T and 5.5 T, respectively. In overall, PMMA-doped MgB$_2$ with different molecular weights of PMMA show substantial enhancement in J_c in the high-field regions both at 5 K and 20 K. This significant enhancement in J_c could be attributed to the effective carbon substitution at boron sites of MgB$_2$ which causes reduction in crystallite size, as evidenced by the increase in the FWHM (not shown here). The small crystallite size results in an increase of density of grain boundaries which act as effective pinning centers for improving $J_c(H)$ properties.

4. CONCLUSION

PMMA polymer was used as a solid carbon source and the effects of its molecular weight on crystal structure, microstructures as well as on superconducting properties of MgB$_2$ were investigated. The decrease in 'a' lattice

PMMA-doped MgB$_2$ samples is most probably due to substitution of C at B sites, as evident by the shrinkage of the 'a' lattice parameter in XRD analysis.

The microstructural FESEM images of (a) undoped and MgB$_2$ doped with different molecular weights of PMMA (b) 350 kg/mol, and (c) 996 kg/mol are presented in Fig. 3. The microstructures of undoped and doped samples look quite similar which consist of well-connected grains network along with porous structure which is typical for MgB$_2$ bulk [11, 12]. The estimation of grain sizes from FESEM images was not possible, therefore, the crystallite sizes were calculated from XRD data and the values are given in Table 1. The pores are mainly developed by
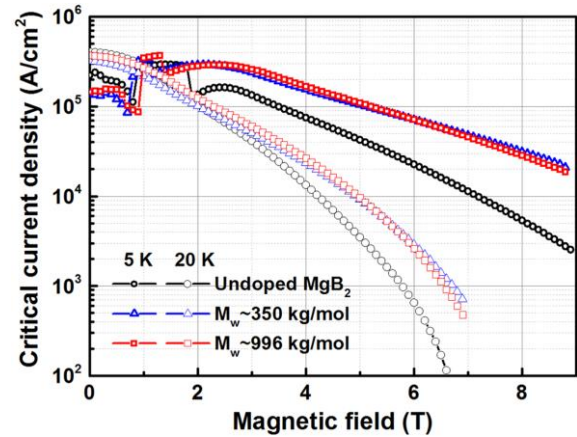
parameter was found for PMMA-doped MgB$_2$ samples, which indicates that the carbon has substituted into boron sites of MgB$_2$ lattice. A systematic decrease in T_c was observed upon lowering the molecular weight of PMMA, which most probably due to increased C substitution. Substantial enhancement in $J_c(H)$ performance was observed for MgB$_2$ doped with different molecular weights of PMMA as compared to undoped MgB$_2$ due to effective carbon substitution at boron sites of MgB$_2$ and the refinement of crystallite size by PMMA doping. We suggest PMMA is a safe and an economical alternative to the explosive gaseous and expensive carbon sources.

ACKNOWLEDGMENT

REFERENCES

[1]   D. Larbalestier, A. Gurevich, D. M. Feldmann, and A. Polyanskii, "High-T_c superconducting materials for electric power applications," *Nature*, vol. 414, pp. 368-377, 2001.

[2]   Mahipal Ranot and W. N. Kang, "MgB$_2$ coated superconducting tapes with high critical current densities fabricated by hybrid physical-chemical vapor deposition," *Curr. Appl. Phys.*, vol. 12, p. 353, 2012.

[3]   S. X. Dou, S. Soltanian, J. Horvat, X. L. Wang, S. H. Zhou, M. Ionescu and H. K. Liu, "Enhancement of the critical current density and flux pinning of MgB$_2$ superconductor by nanoparticle SiC doping," *Appl. Phys. Lett.*, vol. 81, p. 3419, 2002.

[4]   Mahipal Ranot, O. Y. Lee, and W. N. Kang, "Significant enhancement of critical current density by effective carbon-doping in MgB$_2$ thin films," *Prog. Supercond. Cryog.*, vol. 15, pp. 12-15, 2013.

[5]   J. H. Kim *et al.*, "Tailored Materials for High-Performance MgB$_2$ Wire," *Adv. Mater.*, vol. 23, p. 4942, 2011.

[6]   Y. Liu *et al.*, "Significantly enhanced critical current density in nano-MgB$_2$ grains rapidly formed at low temperature with homogeneous carbon doping," *Supercond. Sci. Technol.*, vol. 28, p. 055005, 2015.

[7]   Z. Sun, Z. Yan, J. Yao, E. Beitler, Y. Zhu and J. M. Tour, "Growth of graphene from solid carbon sources," *Nature*, vol. 468, p. 549, 2010.

[8]   G. C. Park, S. M. Hwang, C. M. Lee, J. H. Choi, J. Joo, J. H. Lim, W. N. Kang, C-J Kim, "Improvement of high-field J_c of MgB$_2$ wires by polymethyl-methacrylate doping," *Physica C*, vol. 470, p. S1034, 2010

[9]   M. Avdeev, J. D. Jorgensen, R. A. Ribeiro, S. L. Bud'ko, P. C. Canfield, "Crystal chemistry of carbon-substituted MgB$_2$," *Physica C*, vol. 387, p. 301, 2003.

[10] G. K. Williamson and W. H. Hall, "X-ray line broadening from filed aluminium and wolfram," *Acta Metallurgica*, vol. 1, pp. 22–31, 1953.

[11] V. Grinenko, E. P. Krasnoperov, V. A. Stoliarov, A. A. Bush and B. P. Mikhajlov, "Superconductivity in porous MgB$_2$," *Solid State Commun.*, vol. 456, p. 170, 2007.

[12] M. Ranot, S. H. Jang, Y. S. Oh, K. P. Shinde, S. H. Kang and K. C. Chung, "Addition effects of nanoscale NiO on microstructure and superconducting properties of MgB$_2$," *Prog. Supercond. Cryog.*, vol. 18, pp. 37-40, 2016.

[13] C. J. Kim, J. H. Yi, B. H. Jun, B. Y. You, S. D. Park, K. N. Choo "Reaction-induced pore formation and superconductivity in in situ processed MgB$_2$ superconductors" Physica C., 502, 4–9, 2014.